Astron. Astrophys. 341, 902–911 (1999)

ASTRONOMY
AND
ASTROPHYSICS

Continuum polarization in the solar spectrum

D.M. Fluri and J.O. Stenflo

Institute of Astronomy, ETH Zentrum, CH-8092 Zürich, Switzerland

Received 26 June 1998 / Accepted 2 October 1998

Abstract. We present a theoretical study of the continuum polarization due to radiative scattering in the visible solar spectrum. The results from nine different solar model atmospheres are compared. The center-to-limb variation (CLV) as well as the wavelength dependence of the continuum polarization are determined, and the sources of the dependence on the model atmospheres are identified. The key physical quantities turn out to be the scattering coefficient and the temperature gradient in the layer where the polarization is formed.

A simple analytical function that approximates the CLV of the theoretical continuum polarization for every wavelength in the visible is found. This is based in first approximation on the assumption that the scattering layer producing the polarization is optically thin and lies above the layer of formation of the continuum intensity. Applications of the analytical function range from determinations of the instrumental zero-level of the polarization scale to diagnostic work using empirical center-to-limb curves to constrain the solar model atmospheres.

Key words: polarization – radiative transfer – scattering – Sun: atmosphere – Sun: photosphere

1. Introduction

Recent observations (Stenflo & Keller 1996, 1997) have revealed a richly structured polarization spectrum of the Sun, known as the "second solar spectrum", since it bears little resemblance to the ordinary, unpolarized intensity spectrum and thus contains at least in part complementary information. The structuring is due to mixed contributions of similar importance from the continuum and lines. The continuous spectrum gets linearly polarized by radiative scattering, mainly by Rayleigh scattering at neutral hydrogen and by Thomson scattering at free electrons. The polarization in spectral lines is due to coherent scattering in atomic bound-bound transitions and is altered by the ubiquitous magnetic fields.

In order to fully understand the various physical processes involved we need to disentangle them. In the present paper we start with the continuous spectrum. Apart from a better understanding of the physics such a study is of great use for constraining solar model atmospheres and for the determination of the zero level of the observed polarization scale.

With a solar model atmosphere as input the continuum polarization is obtained by numerically solving the transfer equation for polarized radiation. Different model atmospheres give different degrees of polarization. A comparison with empirical data will therefore enable us to select between several solar model atmospheres. Such observations in continuum windows from 4500 Å to 8000 Å with a sensitivity of 10^{-5} in the degree of polarization are planned but not yet available.

For the diagnostics of turbulent magnetic fields with the Hanle effect it is necessary to know precisely the true zero level of the polarization scale (Stenflo et al. 1998). The Hanle effect, a coherence phenomenon occurring in coherent scattering in the presence of magnetic fields, leads to a depolarization in the line core. Since the polarization in the lines and the continuum are usually of the same order of magnitude one cannot use the continuum level as a reference for line polarization. The true polarization zero level must be the reference. Due to instrumental effects, the true zero point of the polarization scale is not known with sufficient precision. However, knowing the degree of continuum polarization from theoretical considerations, the zero level in the observations can be determined.

In Sect. 2 we will describe the relevant physical theory, the numerical technique, and the solar model atmospheres used. In Sect. 3 two tests of the computer code are presented. In Sect. 4 we gain physical insight into the relevant quantities by illustrating the role of the absorption and scattering coefficients and the temperature gradient. It is of special importance to know the layer of formation of the continuum polarization, since it is often assumed to lie well above the layer of formation of the continuum intensity. We will show that the two layers in fact overlap. Finally, in Sect. 5 a simple analytical expression describing the center-to-limb variation (CLV) of the continuum polarization over the whole visible spectral range is derived and fitted to the theoretical data, providing a convenient approximate representation of the full set of computed polarization values.

Send offprint requests to: D.M. Fluri (dfluri@astro.phys.ethz.ch)

2. Theoretical approach

2.1. Physical processes involved

In order to quantitatively describe radiative transport (see Sect. 2.2) the physical processes have to be understood. Traditionally a distinction is made between pure absorption and scattering (Mihalas 1978). Here we focus on the processes causing the continuous spectrum.

In pure absorption part of the energy of the radiation field is converted into kinetic energy of the gas and thus thermalized. As was first proposed by Wildt (1939), the negative ion of hydrogen H^- dominates the continuous absorption in the solar photosphere, where the visible continuum is formed.

The scattering coefficient in our computer code contains the combined effects of both Thomson scattering at free electrons, which is wavelength independent, and Rayleigh scattering at neutral hydrogen, which obeys the well-known λ^{-4} law. Both processes are coherent. In the scattering process an incident, anisotropic radiation field gets polarized. The anisotropy, a necessary prerequisite for the scattering polarization, is mainly a consequence of the CLV of the intensity, i.e., the limb darkening.

2.2. Formulation of the transfer problem for polarized radiation

We consider a plane-parallel, static atmosphere with homogeneous layers. No magnetic field is included in the calculations. The polarized radiation field is described by the four Stokes parameters I, Q, U and V, as defined for example in Stenflo (1994). If we choose the coordinate system such that Stokes Q represents linear polarization with respect to the direction parallel to the nearest solar limb the above assumptions imply that Stokes U and V are intrinsically zero:

$$U = V \equiv 0 \; . \tag{1}$$

Hence, we can exclude Stokes U and V from our considerations and define the Stokes vector as

$$\boldsymbol{I}_\nu = \begin{pmatrix} I \\ Q \end{pmatrix} \; . \tag{2}$$

We introduce $\mu = \cos\vartheta$, where ϑ is the angle between the direction normal to the surface and the line of sight. The optical depth is defined as

$$d\tau_\nu = -(\kappa_\mathrm{c} + \sigma_\mathrm{c})\, dz \; , \tag{3}$$

z being the geometric height, κ_c the continuum absorption coefficient, and σ_c the scattering coefficient. Polarized radiative transfer in the absence of magnetic fields then is described by the equation

$$\mu \frac{d\boldsymbol{I}_\nu}{d\tau_\nu} = \boldsymbol{I}_\nu - \boldsymbol{S}_\nu \; , \tag{4}$$

with the total source function

$$\boldsymbol{S}_\nu = \frac{1}{(\kappa_\mathrm{c} + \sigma_\mathrm{c})} \left(\kappa_\mathrm{c} \boldsymbol{B}_\nu + \sigma_\mathrm{c} \boldsymbol{S}_{\mathrm{s},\,\nu}\right) \; . \tag{5}$$

The first term in Eq. (5), associated with pure absorption, is determined by the Planck function B_ν and is given by

$$\boldsymbol{B}_\nu = \begin{pmatrix} B_\nu(T) \\ 0 \end{pmatrix} \; . \tag{6}$$

The second term in Eq. (5) contains all radiative sources associated with scattering and can be written as

$$\boldsymbol{S}_{\mathrm{s},\nu}(\mu) = \int \boldsymbol{P}_\mathrm{R}(\mu, \mu') \boldsymbol{I}_\nu(\mu') \, \frac{d\Omega'}{4\pi} \; , \tag{7}$$

where μ' represents the direction of the incident radiation within the differential solid angle $d\Omega'$, and $\boldsymbol{P}_\mathrm{R}$ is the Rayleigh phase matrix, which accounts for the angular dependence of Rayleigh and Thomson scattering. This is given by (Stenflo 1994)

$$\boldsymbol{P}_\mathrm{R} = \boldsymbol{E}_{11} + \tfrac{3}{4} \boldsymbol{P}^2 \; , \tag{8}$$

where $\boldsymbol{E}_{11}$ denotes a matrix with the only non-vanishing element $E_{11} = 1$, representing unpolarized, isotropic scattering, whereas the matrix $\boldsymbol{P}^2$ accounts for linear-polarization scattering and is given by

$$\boldsymbol{P}^2 = \frac{1}{2} \begin{pmatrix} \frac{1}{3}(1-3\mu^2)(1-3\mu'^2) & (1-3\mu^2)(1-\mu'^2) \\ (1-\mu^2)(1-3\mu'^2) & 3(1-\mu^2)(1-\mu'^2) \end{pmatrix} . \tag{9}$$

2.3. Numerical technique

The structure of the computer code is as follows: The most important input is the solar model atmosphere. In the first step the absorption and scattering coefficients, κ_c and σ_c, are calculated while neglecting polarization. This is accomplished by solving the hydrogen radiative transfer problem in non-LTE using the code MULTI by Carlsson (1986). In MULTI κ_c and σ_c are obtained with the opacity package of Gustafsson (1973), taking non-LTE aspects into account. The second step then consists of solving the polarized transfer equation (4) using the previously computed κ_c and σ_c.

For the solution of Eq. (4) a standard technique is used, the so-called Feautrier method. The idea of the Feautrier method is to write the transfer equation for each depth point in the form of a system of second-order differential equations subject to two boundary conditions, one at the top, the other at the bottom of the atmosphere. Integrals are approximated by Gaussian quadrature and differentials by difference formulae, which leads to a set of linear equations with block tridiagonal structure that remains to be solved. A detailed description of the Feautrier method is given by Mihalas (1978).

The following boundary conditions are used: No radiation is entering the atmosphere from above, whereas at the bottom of the atmosphere the diffusion approximation (Mihalas 1978) is applied.

2.4. Solar model atmospheres considered

The nine solar model atmospheres that we have considered are labeled by abbreviations. The number in the subscript indicates the atmospheric model when ordered from the hottest to the

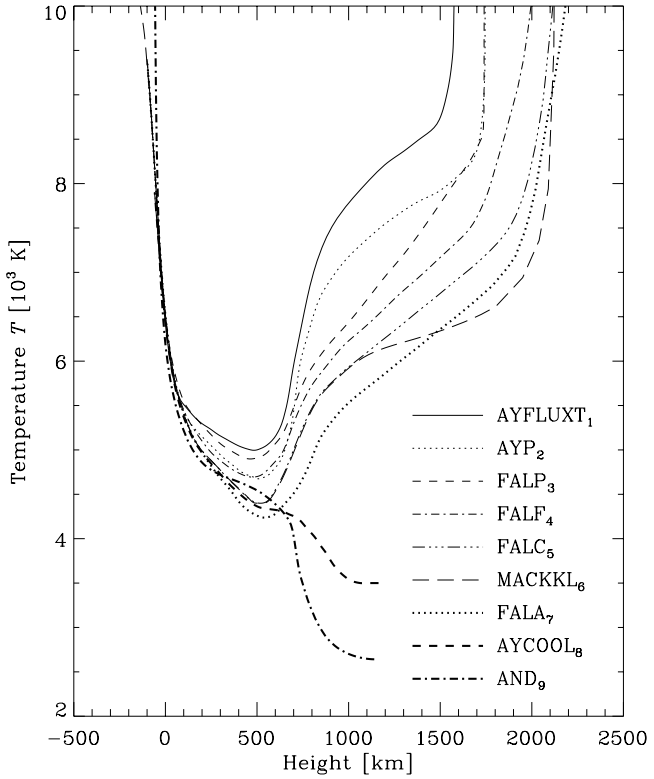

Fig. 1. Temperature as a function of geometric height for the nine solar model atmospheres considered.

coolest atmosphere, as may be seen from Fig. 1, which shows the temperature as a function of geometric height.

- **AYFLUXT$_1$, AYP$_2$, AYCOOL$_8$:** These model atmospheres are based on models introduced by Ayres et al. (1986) and Solanki et al. (1994). AYFLUXT$_1$ is the magnetic component of a plage model, AYP$_2$ a plage model, and AYCOOL$_8$ the non-magnetic component of a plage region.
- **MACKKL$_6$:** This semi-empirical solar model atmosphere, constructed by Maltby et al. (1986), is representative of the average quiet Sun. The temperature as a function of height has been derived from observed CLV curves of the continuous intensity spectrum over a wide wavelength range from X-rays to radio waves.
- **FALA$_7$, FALC$_5$, FALF$_4$, FALP$_3$:** These are models of Fontenla et al. (1993). FALA$_7$ corresponds to their model A, FALC$_5$ to model C, FALF$_4$ to model F, and FALP$_3$ to model P. All models are semi-empirical and include effects of particle diffusion in the transition region to explain UV emission lines of hydrogen and helium correctly. The first three models describe the quiet Sun: FALA$_7$ the supergranular cell center, FALC$_5$ the average quiet Sun, and FALF$_4$ the bright network. FALP$_3$ is a plage model. FALC$_5$ is based on the MACKKL$_6$ atmosphere, but in FALC$_5$ the temperature in the chromosphere has been raised to account for the UV emission lines (see Fig. 1).
- **AND$_9$:** This is model 2 of Anderson (1989). It is a theoretical, non-LTE solar model atmosphere in hydrostatic and radiative equilibrium with plane-parallel geometry. Line blanketing has been included. There is no temperature rise in the chromosphere because non-thermal heating mechanisms are not included in the model. Although on the real Sun the temperature does increase in the chromosphere, this model atmosphere is useful for reference purposes to study the chromospheric influence on polarization.

3. Tests of the computer code

We have performed two tests to check the computer code. The first one, discussed in Sect. 3.1, consists of calculating a special case, namely that of a perfectly scattering atmosphere. As a second test, the theoretical and observed CLV of the continuum intensity are compared in Sect. 3.2.

3.1. Purely scattering atmosphere

Chandrasekhar (1960) has derived the exact solution of the transfer equation for a purely scattering atmosphere in radiative equilibrium, in which the angular dependence of the scattering is controlled by the Rayleigh phase matrix (8). Pure scattering refers to a conservative atmosphere with constant net flux, in which the whole opacity is due to scattering, so no pure absorption occurs. The Stokes $I/I_{\rm center}$, where $I_{\rm center}$ denotes the intensity at disk center, and Q/I components of the continuum radiation field at the top of the atmosphere turn out to be independent of frequency and of all thermodynamic properties because of the lack of thermal coupling between the radiation field and the gas.

We have obtained a purely scattering atmosphere in our calculations in the following way: The scattering coefficient was artificially redefined as the sum of the original $\kappa_{\rm c}$ and $\sigma_{\rm c}$, while the absorption coefficient was set equal to zero. The atmosphere is no longer self-consistent after these redefinitions. Nevertheless, Chandrasekhar's solution should be unrelated to the depth dependence of the temperature, density, and pressure.

All solar model atmospheres do indeed render identical center-to-limb variations of the polarization and the intensity for all wavelengths considered, from 4000 Å to 8000 Å. Moreover, these curves reproduce precisely the exact solution, as seen in Fig. 2. This verifies that scattering has been correctly implemented in the code.

3.2. Comparison with observed limb darkening

Many observers have measured the solar limb darkening. The CLV curves of the intensity so obtained are then fitted to suitable analytical functions or limb-darkening laws, usually containing up to five fit parameters. In general these parameters depend on wavelength.

For the comparison of our calculations with observed CLVs we have chosen the analytical limb-darkening law $L_4(\mu)$ given in Neckel (1996). It is not claimed that the function $L_4(\mu)$ is representative of the Sun, but it is expected to best describe the average quiet Sun. Any new measurement will differ somewhat

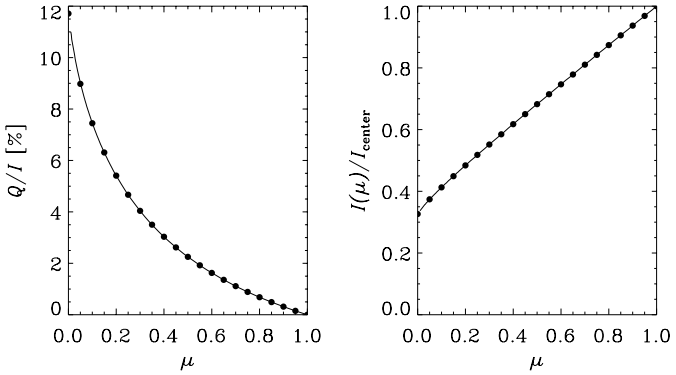

Fig. 2. For the case of pure scattering a comparison is shown between the exact solution (filled circles), given by Chandrasekhar (1960), and our calculations (solid line). The left panel shows the CLV of the polarization and the right panel the limb darkening. All model atmospheres give the same solid lines for all wavelengths from 4000 Å to 8000 Å.

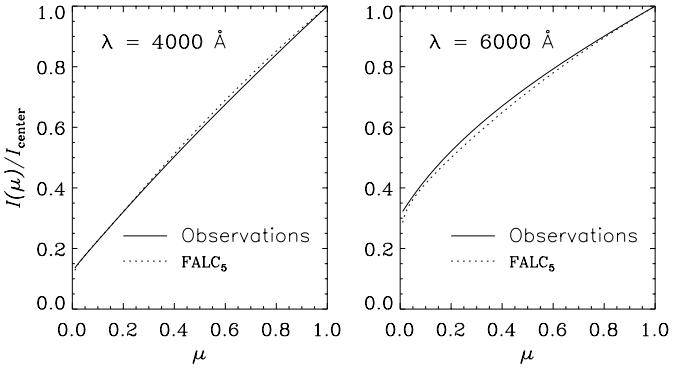

Fig. 3. Comparison of observed limb darkening (Neckel 1996; solid lines) and our calculations (dotted lines) for the average quiet Sun model FALC_5 for two different wavelengths.

from this expression due to the limb-darkening variability. Likewise, it is unlikely that our calculations will perfectly reproduce it. We may however expect the calculated limb darkening of the quiet Sun models to agree reasonably well with the empirical data.

Fig. 3 shows a comparison between the observed (solid line) and the computed limb darkening of FALC_5 for two different wavelengths (note that MACKKL_6 renders the same results as FALC_5). The diagram to the right is representative of the worst case within the spectral range considered. Taking the natural variations in the Sun's actual CLV around the Neckel law into account we can conclude that the limb darkening of the quiet Sun is well reproduced with our code.

4. Behavior of the continuum polarization

We applied the computer code to the nine different model atmospheres introduced in Sect. 2.4. After a presentation of the resulting continuum polarization, we identify the reasons for the wavelength dependence (Sect. 4.1) and for the differences between the various model atmospheres (Sect. 4.2). The scattering coefficient and the temperature gradient turn out to be the most important physical quantities.

Fig. 4 presents the calculated continuum polarization for different model atmospheres as a function of μ (left panel) and wavelength (right panel). Let us now summarize the most significant results:

- The CLV is largely determined by simple geometry since Rayleigh and Thomson scattering act as dipole scattering (cf. Sect. 5.1). Due to axial symmetry the scattering polarization vanishes at disk center for all models.
- With increasing wavelength the polarization decreases steeply, mainly due to the wavelength dependence of the Rayleigh scattering. In Sect. 4.1.2 we will show a further effect due to the wavelength dependence of the Planck function.
- Within each of the model groups $\{\mathrm{AYFLUXT}_1, \mathrm{AYP}_2, \mathrm{AYCOOL}_8\}$ and $\{\mathrm{FALP}_3, \mathrm{FALF}_4, \mathrm{FALC}_5, \mathrm{FALA}_7\}$ the polarization is smaller for hotter atmospheres.
- For the two model atmospheres with no chromosphere, AYCOOL_8 and AND_9, the polarizations are similar to those of the other models. Thus the chromosphere does not seem to be very important for the formation of the polarization. $\mathrm{AYFLUXT}_1$ and AYP_2 are the exceptions to this rule and have small contributions in the chromosphere, as will be shown in Sect. 4.2.
- The two average quiet Sun model atmospheres, FALC_5 and MACKKL_6, differ significantly only in the upper chromosphere. However, their polarizations are almost identical, which again demonstrates the low relevance of the upper chromosphere.

4.1. Wavelength dependence

This section is devoted to a qualitative study of the wavelength dependence of the continuum polarization. The essential points are summarized in Fig. 5. The results obtained below are valid for all models. The following discussion is divided into two parts corresponding to the two most important physical quantities, namely the scattering coefficient and the temperature gradient.

4.1.1. Scattering coefficient

Between 4000 Å and 8000 Å the scattering coefficient decreases by approximately a factor of ten in the photosphere, as shown in panels *b* and *e* of Fig. 5. The wavelength dependence of the scattering coefficient comes from the Rayleigh scattering. A smaller scattering coefficient results in a smaller number of scattering processes per unit volume and therefore in a lower polarization. Furthermore, the difference in σ_c is larger between 4000 Å and 6000 Å than between 6000 Å and 8000 Å, which is well reflected by the steeper decline of the polarization at smaller wavelengths.

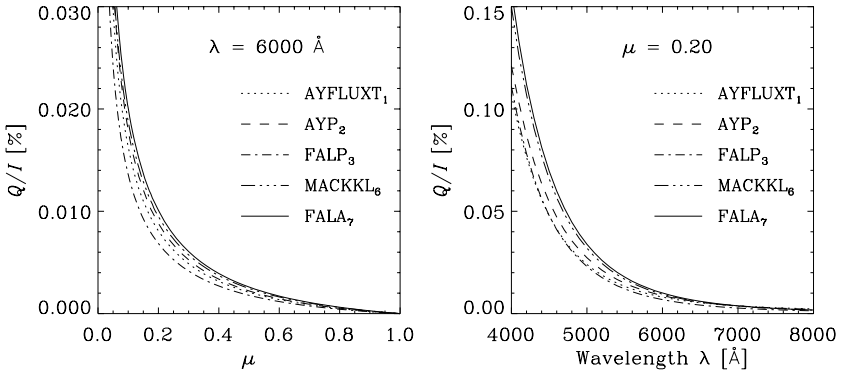

Fig. 4. Center-to-limb variation (*left*) and wavelength dependence (*right*) of the continuum polarization for a representative set of solar model atmospheres. The curves of the other model atmospheres lie between the plotted curves.

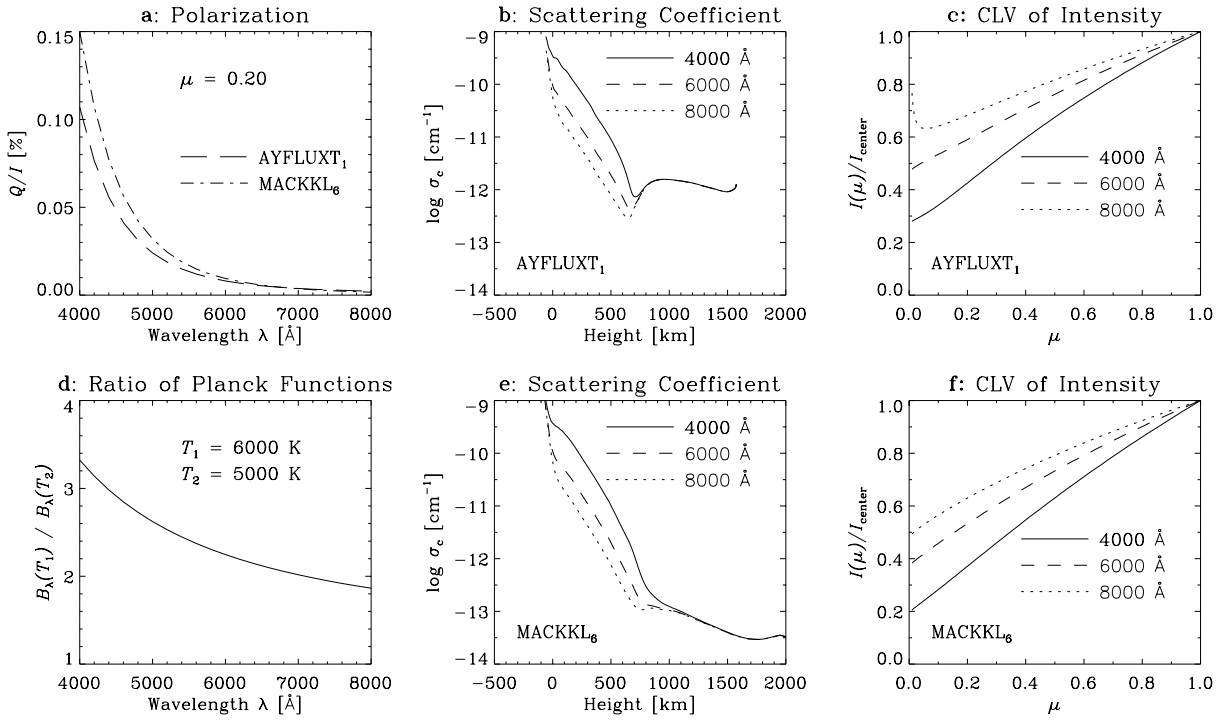

Fig. 5a–f. These plots clarify the causes of the wavelength dependence of the continuum polarization (panel **a**). The two influencing quantities are the scattering coefficient, the logarithm of which is displayed in panels **b** and **e**, and the limb darkening at the height where the contribution function of Stokes Q has a maximum (panels **c** and **f**). Shown are the results for two representative model atmospheres, AYFLUXT$_1$ and MACKKL$_6$. In panel **d** the ratio between two Planck functions with different temperatures is plotted to explain the wavelength dependence of the limb darkening (see text).

4.1.2. Temperature gradient

The temperature gradient is directly responsible for limb darkening. Panels *c* and *f* of Fig. 5 show the CLV of the intensity at the height in the atmosphere where the contribution function (see Sect. 4.2.1) of Stokes Q has a maximum. At this height, which is wavelength and model dependent, the limb darkening is most relevant for the formation of the polarization. This would not be true at the top of the atmosphere, because the formation heights of Stokes I and Q overlap (cf. Fig. 6).

The greater the limb darkening the more anisotropic is the radiation field, and the greater the polarization produced. Fig. 5 clearly shows that the limb darkening decreases with increasing wavelength. This enhances the effect that the scattering coefficient yields a smaller polarization at larger wavelengths.

It is interesting to note the fact that the wavelength dependence of the limb darkening can at least partially be explained by properties of the Planck function, as was pointed out to us by S.K. Solanki (private communication). For simplicity, we assume the absorption coefficient to be wavelength independent and the continuum intensity to be black-body radiation. We consider the Planck function B_λ and fix two temperatures T_1 and T_2 with $T_1 > T_2$. The ratio between two Planck functions, one at temperature T_1, the other at T_2, is given by

$$b_\lambda(T_1,\, T_2) \;=\; \frac{B_\lambda(T_1)}{B_\lambda(T_2)} \;=\; \frac{e^{(hc/\lambda k T_2)} - 1}{e^{(hc/\lambda k T_1)} - 1}\,, \qquad (10)$$

which has the asymptotic values

$$\lim_{\lambda\to\infty} b_\lambda(T_1,\, T_2) \;=\; \frac{T_1}{T_2}\,, \tag{11}$$

$$\lim_{\lambda\to 0} b_\lambda(T_1,\, T_2) \;=\; \infty\,. \tag{12}$$

The ratio b_λ is a monotonically decreasing function of wavelength if $T_1 > T_2$, as shown in panel d of Fig. 5 where b_λ is plotted for two typical temperatures in the photosphere.

In a grey atmosphere the relation between temperature and optical depth is wavelength independent. Therefore the lower value of b_λ at higher wavelengths corresponds to a less pronounced limb darkening, in agreement with panels c and f of Fig. 5. This in turn results in a decreasing polarization with wavelength, even in the case of a grey atmosphere.

4.2. Sources of model dependence

In this section the reasons for the model dependence of the continuum polarization are investigated. Due to the form of the total source function (5) it is natural to examine the influence of the *relative* scattering coefficient

$$\rho = \frac{\sigma_{\rm c}}{\kappa_{\rm c} + \sigma_{\rm c}}\,. \tag{13}$$

This however turns out to be insignificant for explaining the model dependence of the continuum polarization. Rather we find that the temperature gradient in combination with the scattering coefficient, $\sigma_{\rm c}$, appear to be most important, as demonstrated in Fig. 6. Let us now discuss the various quantities plotted in that figure.

4.2.1. Contribution functions

For diagnostic work it is useful to know the location in the atmosphere where the emerging radiation is produced. This information is contained in the *contribution function* $\boldsymbol{C}_z$. To compare the effect of different solar model atmospheres on the polarization we introduce the contribution function with respect to the geometric height z, which is defined by the equation

$$\boldsymbol{I}_\nu(z=\infty,\,\mu) = \int_{-\infty}^{\infty} \boldsymbol{C}_z(z',\,\mu)\,dz'\,. \tag{14}$$

The integration bounds in Eq. (14) are so chosen for formal convenience. However, the errors produced by integrating from minus to plus infinity, instead of only integrating over the atmospheric slab considered, are negligible.

Panel *e* of Fig. 6 displays the contribution functions of Stokes I, $C_{z,\,I}$, and of Stokes Q, $C_{z,\,Q}$, at 6000 Å and $\mu = 0.2$. $C_{z,\,I}$ peaks around a geometric height of 100 km in all models, which shows that the continuum intensity is formed in the lower photosphere. The maximum of $C_{z,\,Q}$ lies higher but still in the photosphere for all models. The fact that the polarization is primarily formed in the photosphere explains the irrelevance of the missing chromosphere in the cool models, AYCOOL_8 and AND_9, and the equality of the polarizations of models FALC_5 and MACKKL_6. Only in the $\mathrm{AYFLUXT}_1$ and AYP_2 atmospheres a relevant part of Stokes Q is produced in the chromosphere, which shows the importance of calculating the opacities in the non-LTE case.

Note that according to the definition (14) the contribution function $C_{z,\,Q}$ is proportional to $\sigma_{\rm c}$ and not to ρ. Therefore, $\sigma_{\rm c}$ is the relevant quantity when interpreting the contribution functions (cf. panels *d* and *e* in Fig. 6).

4.2.2. Relative scattering coefficient

In the photosphere the values of ρ are very similar in all nine model atmospheres (Fig. 6 panel f). Therefore ρ will not cause differences in the polarization between the atmospheres in which Stokes Q is formed in the photosphere. Although $\mathrm{AYFLUXT}_1$ and AYP_2 have a much smaller ρ in the chromosphere, their emergent polarization is not correspondingly reduced. We conclude that ρ is insignificant for explaining the diversity of the continuum polarization in different model atmospheres.

4.2.3. Scattering coefficient

In the photosphere the scattering coefficients are also almost identical in all the model atmospheres and thus do not lead to a model dependence. Only in the cases of $\mathrm{AYFLUXT}_1$ and AYP_2 the chromosphere must not be neglected. Despite the weaker limb darkening of $\mathrm{AYFLUXT}_1$ as compared to AND_9, a significantly higher $\sigma_{\rm c}$ in the chromosphere for the former model results in a correspondingly larger polarization (cf. Fig. 6).

4.2.4. Temperature gradient

According to panel *e* in Fig. 6 the intensity is produced in the photosphere for all model atmospheres. Because the intensity source function is in first approximation equal to the Planck function, the CLV of the continuum intensity is directly related to the temperature gradient, which is confirmed by inspection of panels *b* and *c*: the greater the temperature gradient in the photosphere (approximately between 0 and 500 km) the more pronounced is the limb darkening.

Let us now consider the model atmospheres FALF_4, FALA_7 and AND_9. The differences in $\sigma_{\rm c}$ and ρ are small. However, the limb-darkening curves are not identical and a greater CLV of the intensity corresponds to a higher degree of polarization for these atmospheres.

5. Analytical representation

In order to simplify comparisons with empirical data, we determined an analytical expression, similar to the expression introduced by Stenflo et al. (1997), that approximates the CLV curves of the continuum polarization for all visual wavelengths and all nine solar model atmospheres. Since this function is largely based on physical considerations, it provides us with a better understanding of the formation of the continuum polarization in the solar atmosphere.

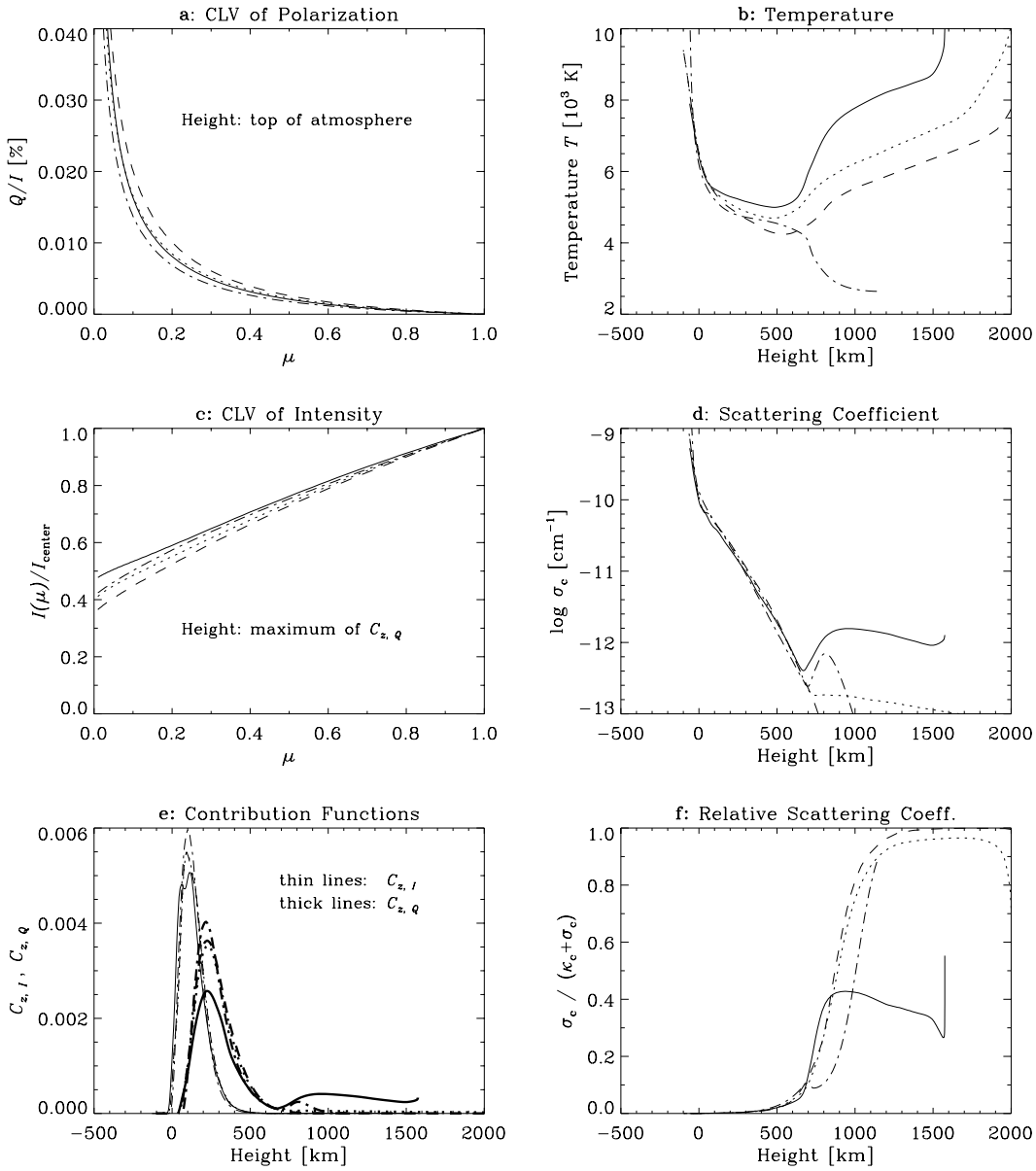

Fig. 6a–f. Illustration of various factors contributing to the differences in the continuum polarization between different model atmospheres: **a**: CLV of the continuum polarization at 6000 Å at the top of the atmosphere. **b**: Temperature as a function of geometric height. **c**: CLV of the continuum intensity relative to the intensity at disk center at the height where $C_{z,\,Q}$ reaches the maximum at 6000 Å. **d**: Logarithm of the scattering coefficient at 6000 Å. **e**: Contribution function of Stokes I ($C_{z,\,I}$, thin lines) and of Stokes Q ($C_{z,\,Q}$, thick lines) at 6000 Å and $\mu = 0.2$. **f**: Relative scattering coefficient at 6000 Å. Description of lines: *solid*: AYFLUXT$_1$; *dotted*: FALF$_4$; *dashed*: FALA$_7$; *dashed-dotted*: AND$_9$.

Here we investigate the applicability and accuracy of our analytical representation. Later our intention is to apply it to observed center-to-limb variations of the continuum polarization to determine the zero level of the polarization scale and to use it for diagnostic work.

5.1. Analytical function

Stenflo et al. (1997) introduced a function that should describe the CLV of the continuum polarization when the scattering layer is optically thin and located above the layer where the major part of the intensity is formed. This function of μ is given by

$$\frac{Q_\lambda}{I_\lambda}(\mu) \;=\; q_\lambda \,\frac{1-\mu^2}{\mu\, I_\lambda(\mu)\,/I_{\lambda,\,\mathrm{center}}}\;, \tag{15}$$

where q_λ is a proportionality constant. However, since the continuum polarization is wavelength dependent, q_λ, being a measure of the degree of polarization, must be a function of wavelength.

Let us summarize the reasons why the particular form of function (15) was chosen. A plane-parallel atmosphere is assumed, in which scattering is confined to a layer above the slab where the intensity is produced. This corresponds to the Schuster-Schwarzschild model (cf. Collins 1989). The path length within the optically thin scattering layer scales as $1/\mu$. The emergent Stokes Q is proportional to the source function for Q, which scales as $(1-\mu^2)$ due to the Rayleigh phase matrix, as can be seen from Eq. (9). These considerations imply that

$$Q(\mu) \sim \frac{(1-\mu^2)}{\mu} \, . \tag{16}$$

Expressed in terms of fractional polarization we then get Eq. (15). The normalization of the intensity in terms of the disk center intensity makes q_λ dimensionless.

In Fig. 6 we have noted that the contribution functions of Stokes I and Q do in fact partly overlap. Test runs have shown that the overlap even increases towards smaller μ values. This indicates that the Schuster-Schwarzschild model is not an ideal characterization. Still, since the peak of the Stokes Q contribution function is located above the point where the maximum of the contribution for Stokes I occurs, we can expect the Schuster-Schwarzschild model to be useful as a first approximation. To correct for higher order deviations we introduce a second parameter m_λ into the function (15) as follows:

$$\frac{Q_\lambda}{I_\lambda}(\mu) \; = \; q_\lambda \, \frac{1-\mu^2}{(\mu + m_\lambda)\, I_\lambda(\mu) \,/ I_{\lambda,\,\mathrm{center}}} \, . \tag{17}$$

As in the case of q_λ, we assume the parameter m_λ to be independent of μ, although it may vary with wavelength.

While the choice of the form (15) has been based on simple physical arguments, the introduction of m_λ is motivated more by mathematical simplicity than by physical reasoning. The physics however enters as follows: We will see in the next section that m_λ is positive and much smaller than unity. Therefore it is only relevant for small μ values and thereby accounts for the fact that the overlap of the Stokes I and Q contribution functions increases for smaller μ, which leads to larger deviations from the simple Schuster-Schwarzschild model. Furthermore the original function (15) diverges for $\mu \to 0$. This is clearly unphysical (Chandrasekhar 1960), since for sufficiently small μ the scattering layer becomes optically thick along the line of sight. The introduction of m_λ improves upon this situation by keeping the polarization at $\mu = 0$ finite as long as m_λ is positive.

We have performed least squares fits of the function (17) to our computations of the polarization CLV. This gives us values for q_λ and m_λ for different wavelengths and model atmospheres. The wavelength and model dependences of the two parameters will be given explicitly below.

Calculations have shown that m_λ, although needed to improve the fit, is fairly insensitive to the choice of model atmosphere. Therefore the function (17) is fitted to the theoretical CLV curves with m_λ fixed. Thus only q_λ is a free, model dependent parameter. In Fig. 7 the parameters q_λ and m_λ are shown as functions of wavelength and model atmosphere.

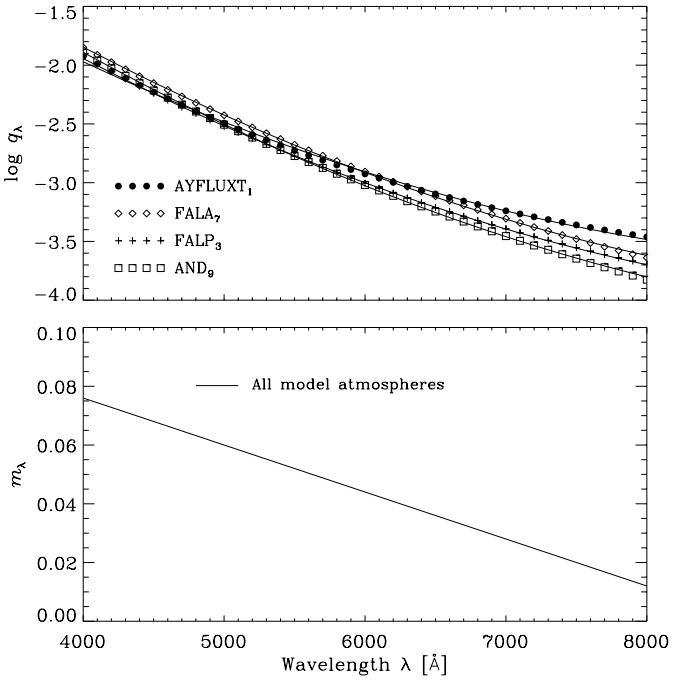

Fig. 7. Wavelength dependence of the parameters q_λ and m_λ, which are used in the analytical function approximating the CLV curves of the continuum polarization. (Note that the logarithm of q_λ is shown.) To avoid overloading the plot we do not show all models. AYP_2 yields a similar curve as $AYFLUXT_1$ while the other model atmospheres lie approximately between the $FALA_7$ and $FALP_3$ curves.

5.2. Wavelength dependence of m_λ

The wavelength dependence of m_λ is well represented by a linear function (see Fig. 7),

$$m_\lambda = b_0 + b_1 \lambda \, , \tag{18}$$

where the coefficients b_i are the same for all models. Their values are listed in Table 1, the wavelength being expressed in Å.

5.3. Wavelength dependence of q_λ

The wavelength dependence of q_λ is best described by the expression

$$\log q_\lambda = a_0 + a_1 \lambda + a_2 \lambda^2 \, . \tag{19}$$

Note that on the left hand side the base-10 logarithm of q_λ is given and not q_λ itself. The coefficients a_i are listed in Table 1, the wavelength being expressed in Å. As for m_λ we have found that it is not necessary to let a_2 freely vary from model to model, but we can keep it at a fixed value for all the models.

It is absolutely necessary to keep all four significant digits of a_i as given in the table. The reason is that the center-to-limb curves obtained by the analytical function are very sensitive to tiny changes in q_λ. Table 1 might give the impression that a_2 could be neglected because it is a factor 10^4 smaller than a_1. However, this huge factor is due to the circumstance that the

Table 1. Coefficients describing the wavelength dependence of the fit parameters q_λ and m_λ (Eqs. (19) and (18)). The wavelength has to be given in units of Å. Note that a_2, b_0, and b_1 are identical for all model atmospheres.

Model	a_0	a_1	a_2	b_0	b_1
$\mathrm{AYFLUXT}_1$	0.9822	$-9.182 \cdot 10^{-4}$	$4.500 \cdot 10^{-8}$	0.140	$-1.60 \cdot 10^{-5}$
AYP_2	1.128	$-9.427 \cdot 10^{-4}$	$4.500 \cdot 10^{-8}$	0.140	$-1.60 \cdot 10^{-5}$
FALP_3	1.253	$-9.789 \cdot 10^{-4}$	$4.500 \cdot 10^{-8}$	0.140	$-1.60 \cdot 10^{-5}$
FALF_4	1.315	$-9.806 \cdot 10^{-4}$	$4.500 \cdot 10^{-8}$	0.140	$-1.60 \cdot 10^{-5}$
FALC_5	1.338	$-9.801 \cdot 10^{-4}$	$4.500 \cdot 10^{-8}$	0.140	$-1.60 \cdot 10^{-5}$
MACKKL_6	1.343	$-9.809 \cdot 10^{-4}$	$4.500 \cdot 10^{-8}$	0.140	$-1.60 \cdot 10^{-5}$
FALA_7	1.368	$-9.834 \cdot 10^{-4}$	$4.500 \cdot 10^{-8}$	0.140	$-1.60 \cdot 10^{-5}$
AYCOOL_8	1.330	$-9.805 \cdot 10^{-4}$	$4.500 \cdot 10^{-8}$	0.140	$-1.60 \cdot 10^{-5}$
AND_9	1.462	$-1.018 \cdot 10^{-3}$	$4.500 \cdot 10^{-8}$	0.140	$-1.60 \cdot 10^{-5}$

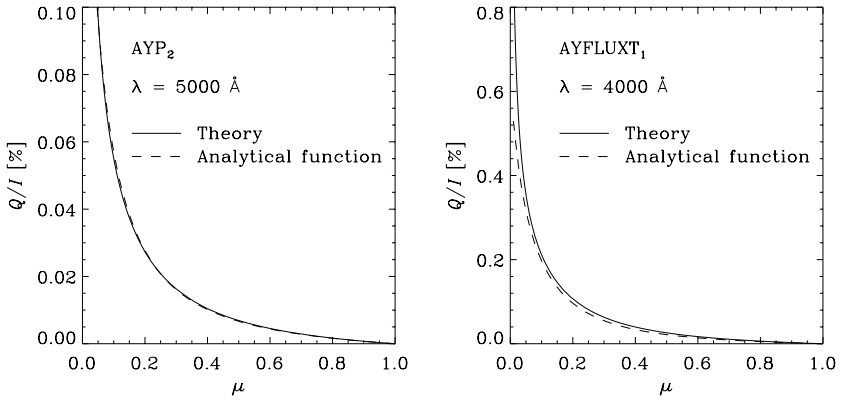

Fig. 8. Comparison between theoretical, computed CLV curves of the continuum polarization and the fitted analytical function of Eq. (17) using the wavelength dependence of the fit parameters given by the coefficients a_i and b_i in Table 1. The left panel is representative of the best fit, while the right panel shows one of the worst fits.

wavelength is measured in Å. The terms containing a_0, a_1 and a_2 in Eq. (19) are indeed of the same order of magnitude.

5.4. CLV curves

We tested Eq. (17) against our computations of the continuum polarization CLV for the different model atmospheres. Fig. 8 shows the results of this test for two different model atmospheres and two fixed wavelengths. The left panel is representative of the best fit whereas the right panel shows one of the worst fits.

The introduction of m_λ has improved the representation of the theoretical data drastically. For most model atmospheres and wavelengths major deviations of the analytical function from the theoretical curve occur only very close to the limb, for $\mu < 0.05$. Since observations that close to the limb (within one arcsec) are very difficult because of seeing, and because the analytical function (17) was introduced primarily to simplify comparisons with observations, we can conclude that the functional form adopted to describe the CLV of continuum polarization is appropriate.

6. Conclusions

We used a computer code that implements the Feautrier method to solve the radiative transfer equation for the polarized radiation in the continuum, which is produced by Rayleigh and Thomson scattering. We have given qualitative physical arguments that explain the dependence on wavelength and model atmosphere of the continuum polarization.

The wavelength dependence is due to the scattering coefficient, which varies according to the known λ^{-4} law for Rayleigh scattering, and to the CLV of the continuum intensity. It is interesting to note that even in a grey atmosphere the polarization is smaller at longer wavelengths because of the properties of the Planck function. For a given temperature difference the relative change of the Planck function decreases monotonically towards longer wavelengths, which results in less steep center-to-limb variations of the intensity.

The model dependence of the continuum polarization is mainly due to the limb darkening and the temperature gradient. The scattering coefficient is less important, because in the photosphere it is almost identical in all models. However, it does play a role in the flux-tube model ($\mathrm{AYFLUXT}_1$) and in one of the plage model atmospheres, where some contribution to the continuum polarization from the chromosphere is present due to a very high scattering coefficient there.

We introduced the analytical function (17) to describe the computed CLV of the continuum polarization for all nine model atmospheres and all visible wavelengths. For $m_\lambda = 0$ this function follows from the simple assumption of an optically thin scattering layer lying above the layer of formation of the continuum intensity. Because our theoretical computations have re-

vealed that this assumption is only partly satisfied, the parameter m_λ has been introduced.

The expression (17) fits well the computed CLV curves of the continuum polarization, which proves the usefulness of this representation. The wavelength variations of both q_λ and m_λ have been given by simple analytical expressions, which allow us to retrieve the CLV of the polarization for all visible wavelengths and for $\mu > 0.05$. Closer to the limb (within the last arcsec) the approximation (17) gets worse.

In future work we plan to measure the continuum polarization in selected windows in the visible part of the solar spectrum. The analytical function would then be fitted to the observed CLV curves. This will allow us to determine the problematic zero point of the polarization scale. The fitted values of q_λ may also be used to constrain the model atmospheres. We further intend to explore the non-linear coupling between the continuum and the lines in order to gain a more complete understanding of the second solar spectrum.

Acknowledgements. We wish to thank Marianne Faurobert-Scholl, who provided us with the heart of the computer code, the Feautrier algorithm, and Sami Solanki for constructive comments on the wavelength dependence of the continuum polarization and for supplying the solar model atmospheres.

References

Anderson, L.S., 1989, ApJ 339, 558
Ayres, T.R., Testerman, L., Brault, J.W., 1986, ApJ 304, 542
Carlsson, M., 1986, Uppsala Astron. Observ. Report, 33
Chandrasekhar, S., 1960, Radiative Transfer, Dover Publications, New York
Collins II, G.W., 1989, The Fundamentals of Stellar Astrophysics, Freeman and Company, New York
Fontenla, J.M., Avrett, E.H., Loeser, R., 1993, ApJ 406, 319
Gustafsson, B., 1973, Uppsala Astron. Observ. Ann. 5(6)
Maltby, P., Avrett, E.H., Carlsson, M., Kjeldseth-Moe, O., Kurucz, R.L., Loeser, R., 1986, ApJ 306, 284
Mihalas, D., 1978, Stellar Atmospheres, Freeman and Company, San Francisco
Neckel, H., 1996, Solar Phys. 167, 9
Solanki, S.K., Livingston, W., Ayres, T., 1994, Sci 263, 64
Stenflo, J.O., 1994, Solar Magnetic Fields, Kluwer, Dordrecht
Stenflo, J.O., Keller, C.U., 1996, Nature 382, 588
Stenflo, J.O., Keller, C.U., 1997, A&A 321, 927
Stenflo, J.O., Bianda, M., Keller, C.U., Solanki, S.K., 1997, A&A 322, 985
Stenflo, J.O., Keller, C.U., Gandorfer, A., 1998, A&A 329, 319
Wildt, R., 1939, ApJ 90, 611